Electronic Supplementary Material (ESI) for Inorganic Chemistry Frontiers.

Insights into the Modulation Mechanisms of Multi-active Sites in Conjugated Small-molecule for Organic Cathodes Capacity from First-principles

Zhaopeng Sun, Hao Tian, Meng Zhang, Yi Zhang, Zhiping Li, Weiwei Huang

Contents

1. Synthesis of 3BQ.

All reagents used in this experiment have been purchased directly without additional purification. As shown in Fig. S1, 3BQ was synthesized by the reaction with Cyclohexanehexone octahydrate ($C_6O_6 \cdot 8H_2O$) and 2,3-Diamino-1,4-naphthoquinone (DANQ).[1] Initially, $C_6O_6 \cdot 8H_2O$ (3.0 g, 9.6 mmol) (1.5g, 4.8 mmol) and DANQ (5.4 g, 28.8 mmol) (2.7g 14.4 mmol) were dissolved in acetic acid/ethanol (1:1/vol.) under the protection of N_2 and refluxed for 24 h. The brown suspension was collected by filtration and washed with hot acetic acid, water, and ethanol. After that, it was stirred with 30% HNO_3 at 140 ℃ for 3 h. Finally, the yellow solid was collected by filtration, washed and dried under a vacuum.

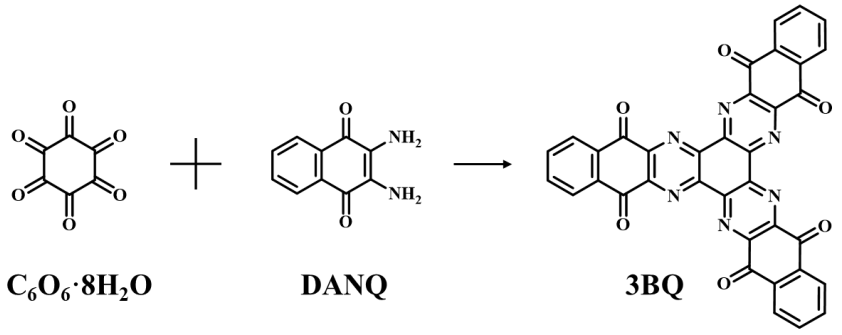

Fig. S1 Synthesis routes of 3BQ.

2. Material characterization of 3BQ.

As shown in Fig. S2 and Fig. S3, the structure of 3BQ was detected by Fourier transforms infrared spectroscopy and ^{1}H nuclear magnetic resonance.

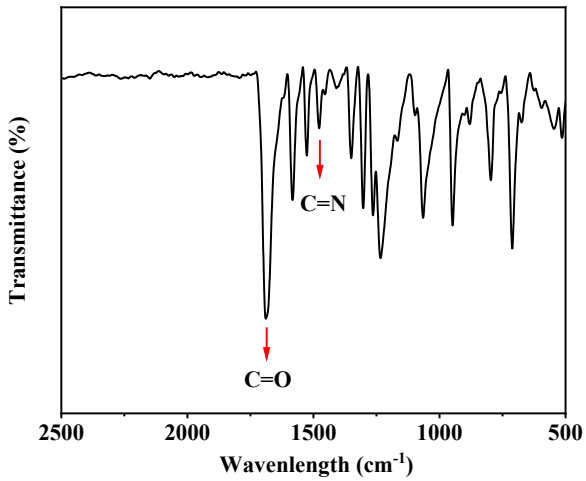

Fig. S2 The FTIR spectrum of 3BQ.

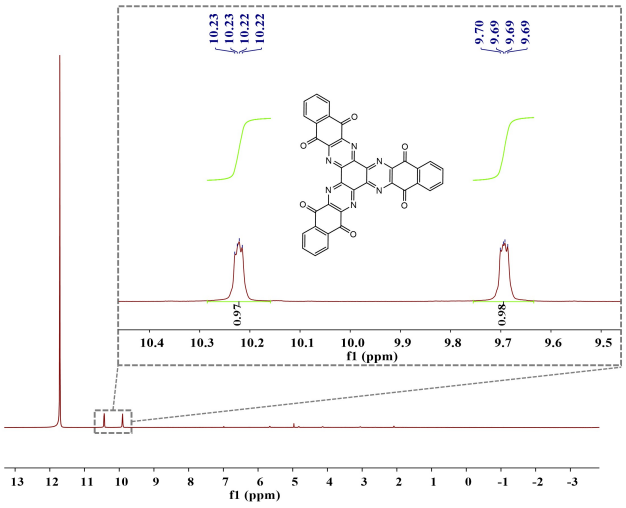

Fig. S3 The ^{1}H NMR spectrum of 3BQ.

3. The theoretical calculations about 3BQ.

Table. S1 Lattice parameters and atomic coordinates of the simulated bilayer 3BQ.

a=15.4581 Å, b=15.4587 Å, c=6.5173 Å α=γ= 90°, β=120°							
Symbol	X	Y	Z	Symbol	X	Y	Z
C1	0.89243	0.94528	0.72339	C61	0.42518	0.47779	0.72255
C2	0.05477	0.94722	0.72338	C62	0.52196	0.94732	0.72256
C3	0.05298	0.10770	0.72340	C63	0.05265	0.57469	0.72256
C4	0.94570	0.89231	0.72308	C64	0.47723	0.42554	0.72315
C5	0.94665	0.05435	0.72309	C65	0.94828	0.52254	0.72315
C6	0.10784	0.05354	0.72309	C66	0.57433	0.05168	0.72316
C7	0.77426	0.38807	0.22628	C67	0.24151	0.85558	0.22710
C8	0.61188	0.38610	0.22626	C68	0.14470	0.38602	0.22711
C9	0.61369	0.22560	0.22624	C69	0.61402	0.75862	0.22711
C10	0.72097	0.44104	0.22660	C70	0.18948	0.90784	0.22650
C11	0.72003	0.27898	0.22658	C71	0.71838	0.81075	0.22652
C12	0.55881	0.27976	0.22653	C72	0.09231	0.28166	0.22651
C13	0.74569	0.79792	0.72405	H1	0.43811	0.62377	0.72235
C14	0.20205	0.94785	0.72402	H2	0.37587	0.81423	0.72237
C15	0.05235	0.25437	0.72407	H3	0.18579	0.56195	0.72238
C16	0.79853	0.74513	0.72276	H4	0.62301	0.43776	0.72259
C17	0.94665	0.20144	0.72278	H5	0.81466	0.37667	0.72259
C18	0.25495	0.05353	0.72273	H6	0.56232	0.18534	0.72259
C19	0.92100	0.53548	0.22573	H7	0.22856	0.70958	0.22734
C20	0.46456	0.38545	0.22570	H8	0.29081	0.51911	0.22732
C21	0.61436	0.07894	0.22570	H9	0.48088	0.77138	0.22734
C22	0.86813	0.58826	0.22697	H10	0.04371	0.89566	0.22702
C23	0.72007	0.13189	0.22695	H11	0.85203	0.95661	0.22703
C24	0.41167	0.27975	0.22693	H12	0.10426	0.14796	0.22699
C25	0.63366	0.74384	0.72516	H13	0.34397	0.43708	0.72242
C26	0.25601	0.88984	0.72515	H14	0.56258	0.90677	0.72244
C27	0.11028	0.36640	0.72518	H15	0.09316	0.65590	0.72243
C28	0.74390	0.63311	0.72172	H16	0.43626	0.34431	0.72341
C29	0.88923	0.25598	0.72172	H17	0.90798	0.56343	0.72341
C30	0.36700	0.11090	0.72167	H18	0.65556	0.09194	0.72344
C31	0.03302	0.58956	0.22464	H19	0.32271	0.89628	0.22716
C32	0.41061	0.44347	0.22460	H20	0.10409	0.42657	0.22717
C33	0.55641	0.96690	0.22462	H21	0.57351	0.67741	0.22717
C34	0.92278	0.70029	0.22785	H22	0.23047	0.98907	0.22616
C35	0.77749	0.07733	0.22787	H23	0.75866	0.76984	0.22617
C36	0.29961	0.22239	0.22783	H24	0.01108	0.24143	0.22617
C37	0.58136	0.63400	0.72314	N1	0.79252	0.89706	0.72432

C38	0.36587	0.94736	0.72313	N2	0.10290	0.89550	0.72430
C39	0.05271	0.41862	0.72315	N3	0.10469	0.20761	0.72433
C40	0.63411	0.58127	0.72264	N4	0.89778	0.79227	0.72266
C41	0.94718	0.36578	0.72266	N5	0.89450	0.10219	0.72268
C42	0.41871	0.05288	0.72262	N6	0.20789	0.10568	0.72266
C43	0.08533	0.69940	0.22668	N7	0.87417	0.43633	0.22539
C44	0.30076	0.38595	0.22666	N8	0.56373	0.43779	0.22538
C45	0.61399	0.91469	0.22668	N9	0.56201	0.12569	0.22534
C46	0.03258	0.75213	0.22712	N10	0.76888	0.54108	0.22699
C47	0.71952	0.96753	0.22714	N11	0.77218	0.23114	0.22697
C48	0.24790	0.28042	0.22711	N12	0.45874	0.22762	0.22691
C49	0.47705	0.58149	0.72256	O1	0.58861	0.79050	0.72818
C50	0.41825	0.89549	0.72258	O2	0.20923	0.79807	0.72822
C51	0.10453	0.52293	0.72257	O3	0.20206	0.41157	0.72822
C52	0.58100	0.47702	0.72286	O4	0.79012	0.58738	0.71999
C53	0.89598	0.41878	0.72286	O5	0.79722	0.20969	0.71996
C54	0.52297	0.10403	0.72286	O6	0.41289	0.20289	0.71990
C55	0.18964	0.75188	0.22718	O7	0.07806	0.54288	0.22162
C56	0.24841	0.43785	0.22716	O8	0.45741	0.53523	0.22153
C57	0.56214	0.81038	0.22718	O9	0.46463	0.92173	0.22156
C58	0.08570	0.85639	0.22683	O10	0.87657	0.74603	0.22917
C59	0.77071	0.91452	0.22685	O11	0.86949	0.12361	0.22923
C60	0.14363	0.22928	0.22682	O12	0.25371	0.13040	0.22917

The crystallographic data (CCDC 1996183) was obtained free of charge from the Cambridge Crystallographic Data Centre *via* www.ccdc.cam.ac.uk/data_request/cif.

Table. S2 Adsorption energies of various possible Na-adsorption sites on molecules in the upper layers of the 3BQ crystal.

Na-adsorption site number	**1**	**2**	**3**	**4**	**5**	**6**
Adsorption energy (eV)	−2.75	−2.74	−2.75	−2.74	−2.74	−2.74
Na-adsorption site number	**7**	**8**	**9**	**10**	**11**	**12**
Adsorption energy (eV)	−1.62	−1.63	−1.61	−1.53	−1.51	−1.52

Table. S3 Adsorption energies of various possible Na-adsorption sites on molecules in the lower layers of the 3BQ crystal.

Na-adsorption site number	**13**	**14**	**15**	**16**	**17**	**18**
Adsorption energy (eV)	−2.75	−2.77	−2.76	−2.78	−2.81	−2.78
Na-adsorption site number	**19**	**20**	**21**	**22**	**23**	**24**
Adsorption energy (eV)	−2.35	−2.37	−2.33	−1.46	−1.60	−1.47

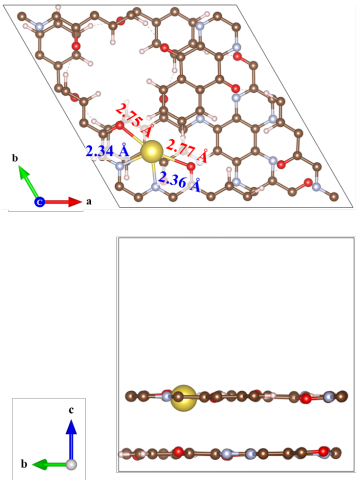

Fig. S4 Front and side views of a single Na^+ adsorbed at the monolayer 3BQ redox center.

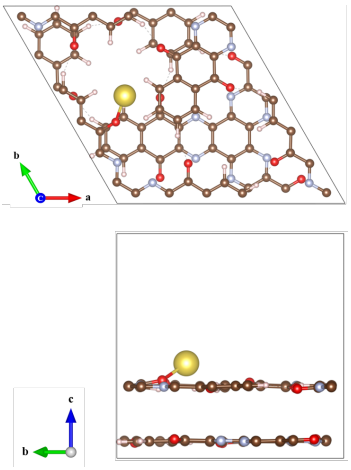

Fig. S5 Front and side views of a single Na^+ adsorbed on the C=O group on the surface of monolayer 3BQ.

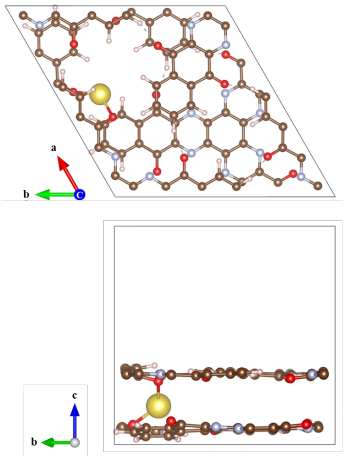

Fig. S6 Front and side views of a single Na^+ adsorbed on the C=O group between monolayer 3BQ layers.

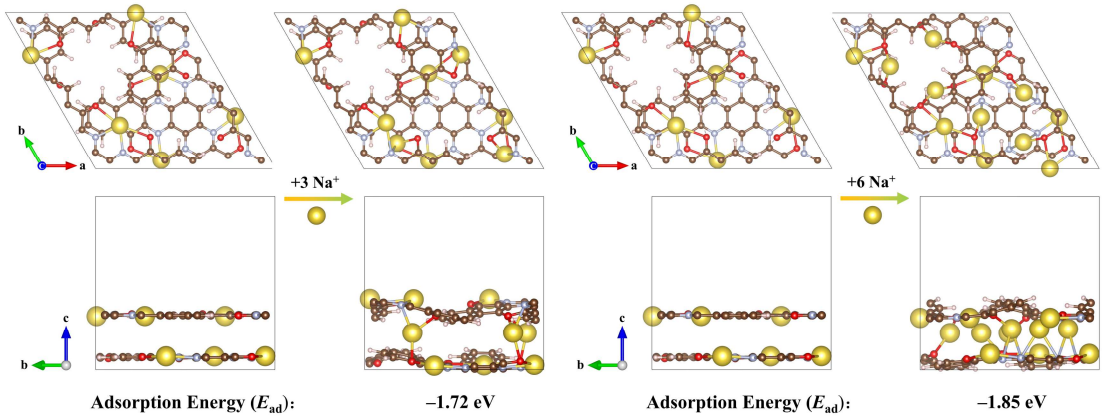

Fig. S7 Average E_{ad} of individual Na^+ corresponding to multiple Na^+ adsorbed between redox sites and adsorbed on the C=O group of 3BQ-3Na.

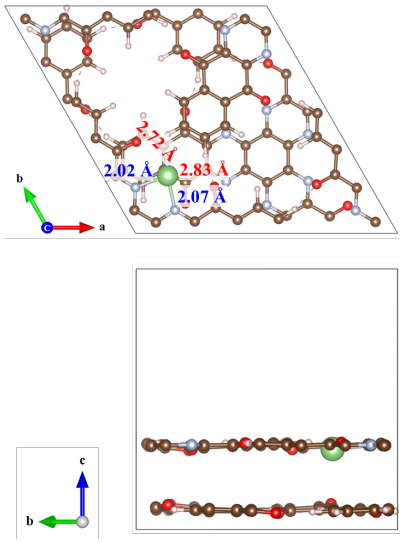

Fig. S8 Front and side views of a single Li^+ adsorbed at the monolayer 3BQ redox center.

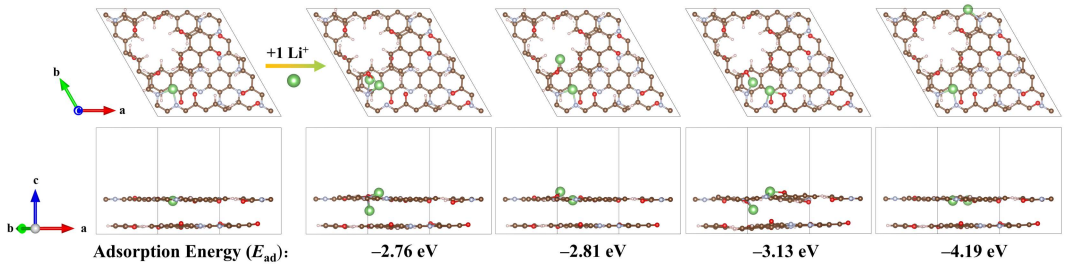

Fig. S9 E_{ad} of potential 2nd Li-adsorption sites on bilayer 3BQ.

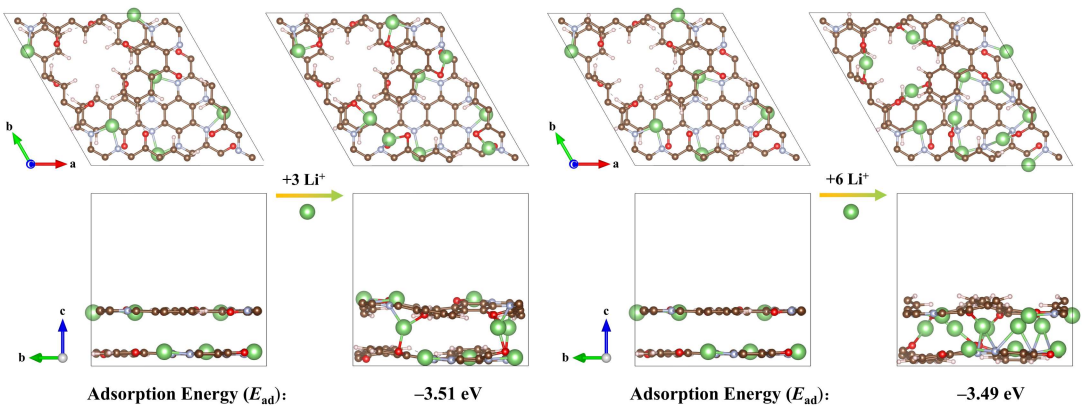

Fig. S10 Average E_{ad} of individual Li^+ corresponding to multiple Li^+ adsorbed between redox sites and adsorbed on the C=O group of 3BQ-3 Li.

4. Electrochemical measurements.

The electrodes were composed of 3BQ (active material), Ketjen black (conductive carbon), and polyvinylidene fluoride (PVDF) (binder) with a mass ratio of 5:4:1. The electrode slurry was prepared using N-methyl-2-pyrrolidinone (NMP) as the solvent and coated onto the aluminum foil current collector. The CR2032 coin cells were assembled with sodium as the counter electrode, 1 M $NaPF_6$ in Diethylene glycol dimethyl ether (DIGLYME) as the electrolyte, and glass microfibers (Whatman GF/D) as a separator in a glovebox with H_2O and O_2 levels below 0.1 ppm. The cyclic voltammetry (CV) was implemented on a CHI instrument electrochemical workstation (CHI-660E).[2, 3] To evaluate the capacity contribution of conductive carbon, a pure Ketjen black electrode (Ketjen black: PVDF = 9:1) were also conducted.

Depending on the maximum possible number of adsorbed Na atoms of the above three stages, the maximum theoretical capacity (C_{theo}) was calculated by

$$C_{theo} = \frac{x\mathrm{F}}{\mathrm{M}_{3BQ}}$$

where x represents the number of electrons involved in the electrochemical process, F is the Faraday constant, and M_{3BQ} is the molecule mass of 3BQ.[4]

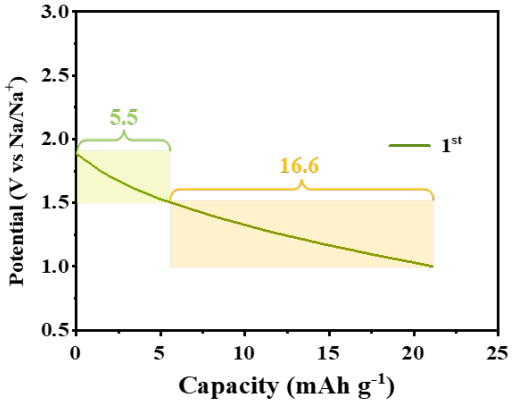

Fig. S11 The 1st discharge curve of conductive carbon at the current density of 100 mA g^{-1}.

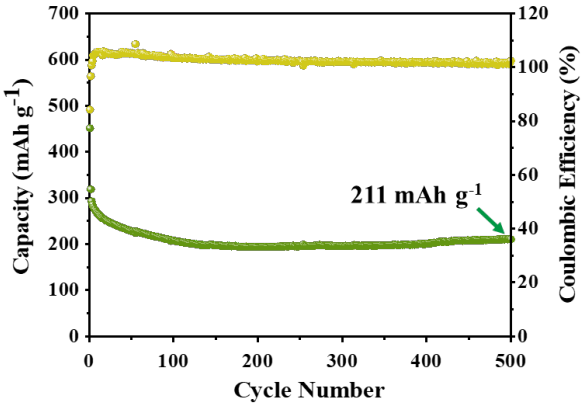

Fig. S12 Cycling stability of 3BQ cathode in NIBs.

References

1. Lee J, Kim H, Park M. J. Long-Life, High-Rate Lithium-Organic Batteries Based on Naphthoquinone Derivatives. *Chem Mat*, 2016, **28**, 2408–2416.
2. Nan T, Yang J, Chen B. Electrochemical mechanism of tin membrane electrodeposition under ultrasonic waves. *Ultrason Sonochem*, 2018, **42**,731–737.
3. Hu Q, Yang J, Nan T, Xie X, Ye Y. Study on the electrically enhanced process for cadmium removal by a pulse in a sulfuric acid system. *Process Saf Environ Protect*, 2022, **159**, 944–952.
4. Wang X, Wang L, Li Y. Prediction of SiS_2 and $SiSe_2$ as promising anode materials for sodium-ion batteries. *Phys Chem Chem Phys*, 2022, **24**, 13189–13193.